

## Reply to “Comment on ‘Gain-assisted superluminal propagation and rotary drag of photon and surface plasmon polaritons’”

Naveed Khan,<sup>1</sup> Bakht Amin Bacha,<sup>2</sup> Azmat Iqbal,<sup>3,\*</sup> Amin Ur Rahman,<sup>3</sup> and A. Afaq<sup>4</sup>

<sup>1</sup>Department of Physics, The University Of Lahore, Lahore, Pakistan

<sup>2</sup>Department of Physics, University of Malakand Chakdara, Dir(L), Pakistan

<sup>3</sup>Faculty of Engineering and Applied Sciences, Department of Physics, Riphah International University, Islamabad 44000, Pakistan

<sup>4</sup>Center of Excellence in Solid State Physics, University of the Punjab, Lahore, Pakistan



(Received 14 January 2019; published 23 May 2019)

Hereby, we amend several spectral parameters reported in our earlier work [N. Khan *et al.*, *Phys. Rev. A* **96**, 013848 (2017); **96**, 049906(E) (2017)], which led to unphysical predictions to be tested experimentally. In particular, the resulting probe wavelength was in the decimeter band, as pointed out in a Comment by Macke and Ségard [B. Macke and B. Ségard, preceding Comment, *Phys. Rev. A* **99**, 057801 (2019)]. After incorporating the corrected parameters, the predictions of our theoretical demonstration on the gain-assisted superluminal propagation and rotary drag of photon and that of surface plasmon polaritons are improved to a good degree of accuracy and expected to be tested realistically. In particular, even the minimum values of rotary drag for both photon and surface plasmon polaritons are on the order of few microradians, thus falling within the range of experimental testability.

DOI: [10.1103/PhysRevA.99.057802](https://doi.org/10.1103/PhysRevA.99.057802)

### I. INTRODUCTION

Recently, we presented theoretical analysis on the gain-assisted superluminal propagation and rotary drag of photons and surface plasmon polaritons (SPPs) by considering a four-level atomic scheme alone (for photons) and coupled with a metallic medium (for SPPs) [1,2]. This Reply is aimed at amending several spectral parameters reported in the earlier work which led to unphysical effects. In particular, the reported value of probe frequency  $\nu_p = 1000\gamma$ , where  $\gamma = 1$  MHz, rendered the probe wavelength falling in the decimeter band (30 cm), as pointed out by Macke and Ségard in the preceding Comment [3]. This in turn led to an absolute susceptibility  $\chi$  on the order of  $10^{12}$ , which can be calculated from Eq. (5) of Ref. [2],

$$\chi^{(2)} = \frac{3N\lambda^3}{32\pi^3\Omega_p} \rho_{ac}^{(2)} = u_\chi \rho_{ac}^{(2)} / \Omega_p, \quad (1)$$

where  $u_\chi = \frac{3N\lambda^3}{32\pi^3}$  [Eq. (4) of the preceding Comment [3]], which also increased to the order of  $4 \times 10^{14}$ . However, as correctly pointed out by Macke and Ségard, the typical value of  $u_\chi$  for physical systems is on the order of  $3 \times 10^{-3}$ .

Retaining the same atomic number density  $N = 5 \times 10^{12} \text{ cm}^{-3}$ , the probe wavelength  $\lambda_p = 2\pi c / \omega_{ac}$  is corrected to be 589.6 nm, where  $\omega_{ac}$  is the corresponding angular frequency of the transition between the states  $|a\rangle$  and  $|c\rangle$  [see Fig. 1(a) in [1]]. In order to satisfy the condition of rotary drag and to overcome the problem of gain instability of the medium, we have reduced the length of the medium to 50  $\mu\text{m}$ . In addition, the corrected SI units for  $\gamma$  and the refractive

index are  $2\pi \times 1$  MHz and  $n = \sqrt{1 + \chi}$ , respectively. Consequently, as expected for realistic systems, the value of  $u_\chi$  with corrected parameters turned out to be  $3.10 \times 10^{-3}$ . In addition to this, for better propagation of SSPs along the metal-dielectric interface [see Fig. 1(b) in [1]], the medium of low conductivity  $\sigma(S/m)$  is replaced with a more conductive one in the revised version (see Figs. 4–8).

### II. NUMERICAL SIMULATIONS AND RESULTS

Hereby, after the aforementioned corrections, we report on the modified numerical results based on the original mathematical formalism presented in [1,2].

Again, one can see a clear gain doublet in the imaginary part of susceptibility  $\text{Im}(\chi)$  plotted with respect to probe detuning in Fig. 1(a). The minimum value of  $\text{Im}(\chi)$  is  $-2.3 \times 10^{-3}$ , where the negative value shows the gain of the probe field in the medium. The corresponding dispersion spectrum is shown by the real part of susceptibility  $\text{Re}(\chi)$  in Fig. 1(b). The anomalous dispersion between the gain doublet supports the superluminal propagation.

The variation of group index and rotatory photon drag  $\theta_r$  with respect to  $\Omega_c/\gamma$  is elaborated in Fig. 2. The maximum negative value of the group index  $n_g$  equals  $6.296 \times 10^6$  at  $\Omega_c/\gamma = 7.55$  and  $\Omega_1 = 8.5\gamma$  (black dotted line). The negative group index manifests superluminal light propagation with a small negative group velocity of 47.65 m/s. The corresponding value of photon drag in Fig. 2(b) is on the order of  $\pm 2.099 \times 10^{-5}$  rad. In Fig. 2(b), positive and negative photon drag results from the counterclockwise and clockwise rotation of the medium, respectively, at the same rotation speed of  $\omega_s = 20$  rps.

\*Corresponding author: [azmatiqbal786@gmail.com](mailto:azmatiqbal786@gmail.com)

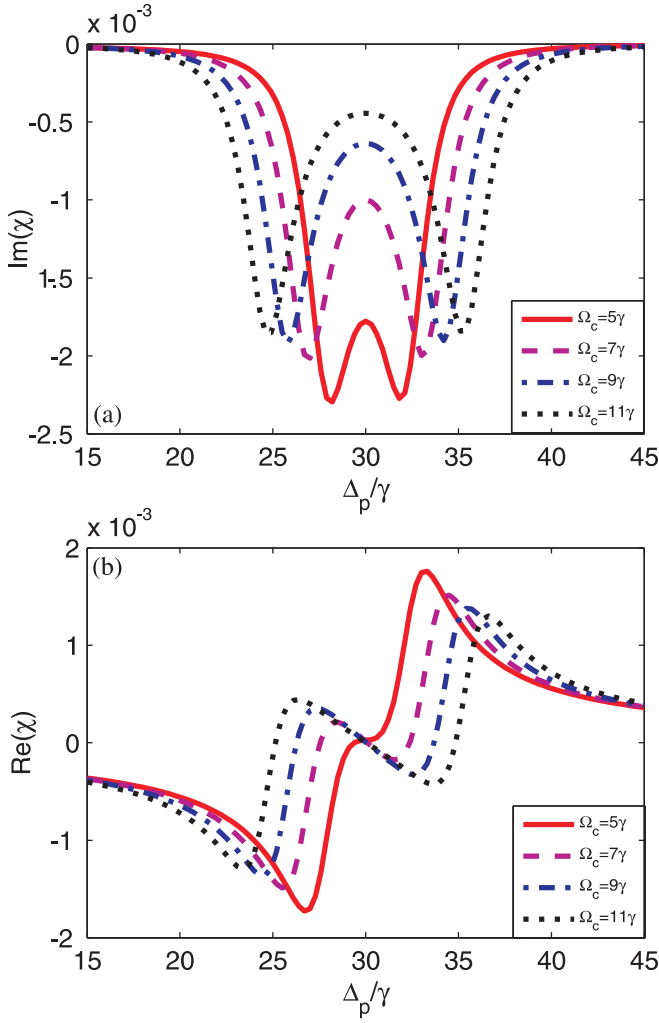


FIG. 1. Variation of complex susceptibility  $\chi$  (in units of  $2N|Q_{ac}|^2/\epsilon_0\hbar$ ) with  $\Delta_p/\gamma$  for (a) the imaginary part and (b) the real part of  $\chi$ . The chosen spectral parameters are  $\gamma = 2\pi \times 1$  MHz,  $\Omega_c = 5\gamma$  (red solid line),  $\Omega_c = 7\gamma$  (magenta dashed line),  $\Omega_c = 9\gamma$  (blue dash-dotted line),  $\Omega_c = 11\gamma$  (black dotted line),  $\gamma_{ac,ad,bd} = 2.5\gamma$ ,  $\gamma_{ab,cd} = 0.5\gamma$ , and  $\Omega_1 = 2.5\gamma$ .

Figure 3 elucidates the variation of rotary photon drag with respect to the rotation speed of the medium. The maximum value of the photon drag is about  $\pm 9.438 \times 10^{-6}$  rad at the medium's rotation speed  $\omega_s = \mp 20$  rps. As one can see, the rotary photon drag  $\theta_r$  is zero for a stationary medium while its value increases linearly with rotation speed. However, rotary photon drag takes place opposite the rotation of the medium; that is, when the medium rotates clockwise, the photon drag is counterclockwise and vice versa. This can be observed from the opposite signs for  $\theta_r$  and  $\omega_s$  during clockwise and counterclockwise rotation of the medium.

As shown in Fig. 4(a), the imaginary part of the wave vector  $\text{Im}(k_{sp})$  of the SPP changes from zero to  $-1.515 \times 10^5$  by increasing  $\Omega_1$  from  $1\gamma$  to  $10\gamma$ . The negative absorption shows the gain-assisted propagation of the SPP along the interface stemming from the negative group index as can be seen in Fig. 5(a). The corresponding change in the real part of  $\text{Re}(k_{sp})$  for the SPP is very small and increases from

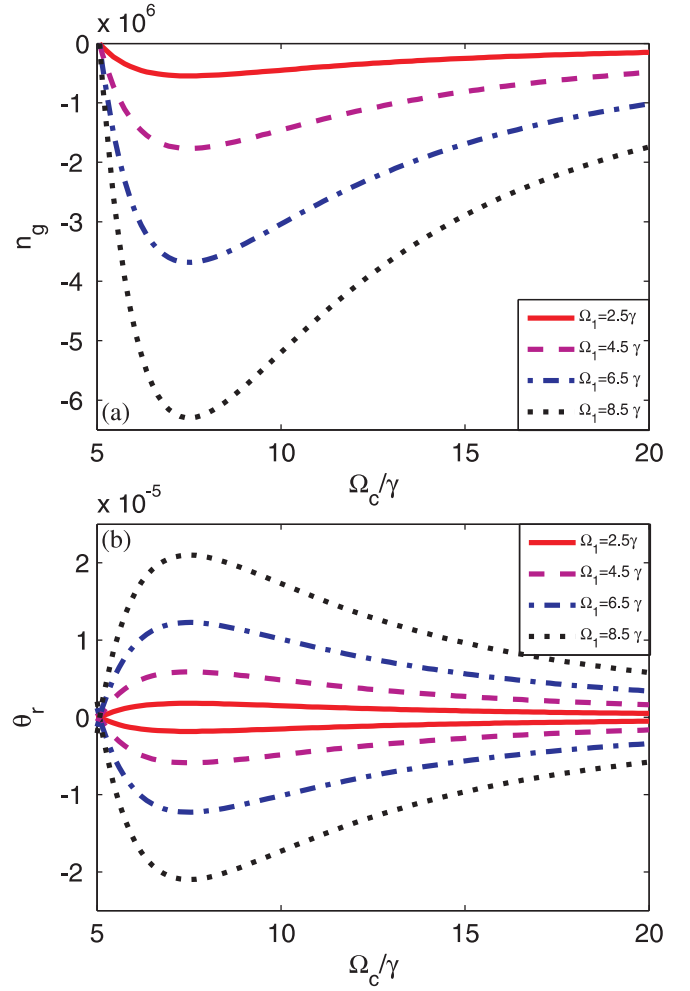


FIG. 2. Variation of the group index  $n_g$  (in units of  $2N|Q_{ac}|^2/\epsilon_0\hbar$ ) and rotary photon drag  $\theta_r$  (in radians) with the control field Rabi frequency  $\Omega_c$  for (a) the group index and (b) the rotary photon drag. The other spectral parameters are  $\Omega_1 = 2.5\gamma$  (red dashed line),  $\Omega_1 = 4.5\gamma$  (magenta dashed line),  $\Omega_1 = 6.5\gamma$  (blue dash-dotted line),  $\Omega_1 = 8.5\gamma$  (black dotted line),  $\gamma_{ac,ad,bd} = 2.5\gamma$ ,  $\gamma_{ab,cd} = 0.5\gamma$ ,  $L = 50 \mu\text{m}$ , and  $\omega_s = \pm 20$  rps.

$1.0657 \times 10^7$  to  $1.0660 \times 10^7$ , within the same change in  $\Omega_1$ . The real part of the wave vector of the SPP describes its dispersion in the medium.

We demonstrate in Figs. 5(a) and 5(b) the dependence of the group index  $n_g^{sp}$  and rotary drag of the SPP  $\theta_r^{sp}$  [Eq. (12) in Ref. [1]] on  $\Omega_1/\gamma$  for various fixed values of the control field Rabi frequency  $\Omega_c$  and other spectral parameters, viz.,  $\Delta_p$ ,  $\Delta_1$ ,  $\omega_s$ ,  $\gamma_{ij}$ , and  $\sigma$ . The maximum negative value of the group index is  $6.803 \times 10^5$  at  $\Omega_1/\gamma = 10$  and  $\Omega_c = 7\gamma$  (magenta dashed line). Analogous to photon drag, the negative value of SPP rotary drag implies that the polarization state of the SPP also rotates opposite the rotation of the dielectric-metal interface. The light propagation switches from its subluminal behavior at the control field  $\Omega_c = 5\gamma$  to the superluminal one at  $7\gamma$ ,  $9\gamma$ , and  $11\gamma$ . Figure 5(a) clearly explicates a noticeable enhancement in  $n_g^{sp}$  by increasing  $\Omega_1$  at various fixed values of  $\Omega_c$ . The corresponding rotary drag of the SPP is demonstrated in Fig. 5(b). The maximum value of rotary drag of

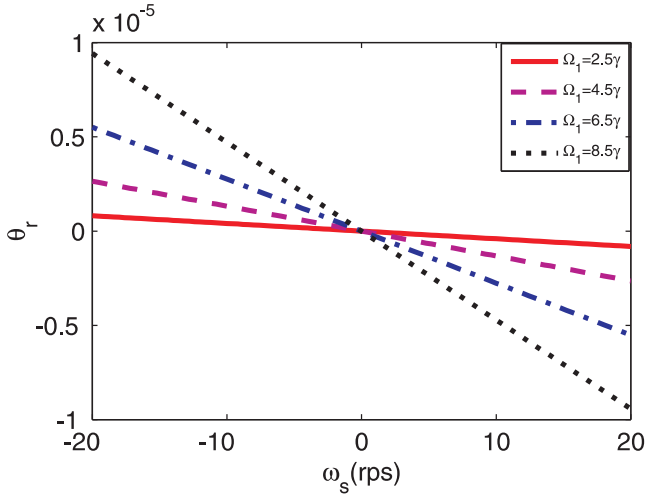


FIG. 3. Dependence of rotary photon drag on rotation speed of the gain-assisted atomic medium. The spectral parameters are  $\Omega_1 = 2.5\gamma$  (red solid line),  $\Omega_1 = 4.5\gamma$  (magenta dashed line),  $\Omega_1 = 6.5\gamma$  (blue dash-dotted line),  $\Omega_1 = 8.5\gamma$  (black dotted line),  $\Omega_3 = 5.5\gamma$ ,  $\Delta_{p,1} = 30\gamma$ ,  $\gamma_{ac,ad,bd} = 2.5\gamma$ ,  $\gamma_{ab,cd} = 0.5\gamma$ , and  $L = 50 \mu\text{m}$ .

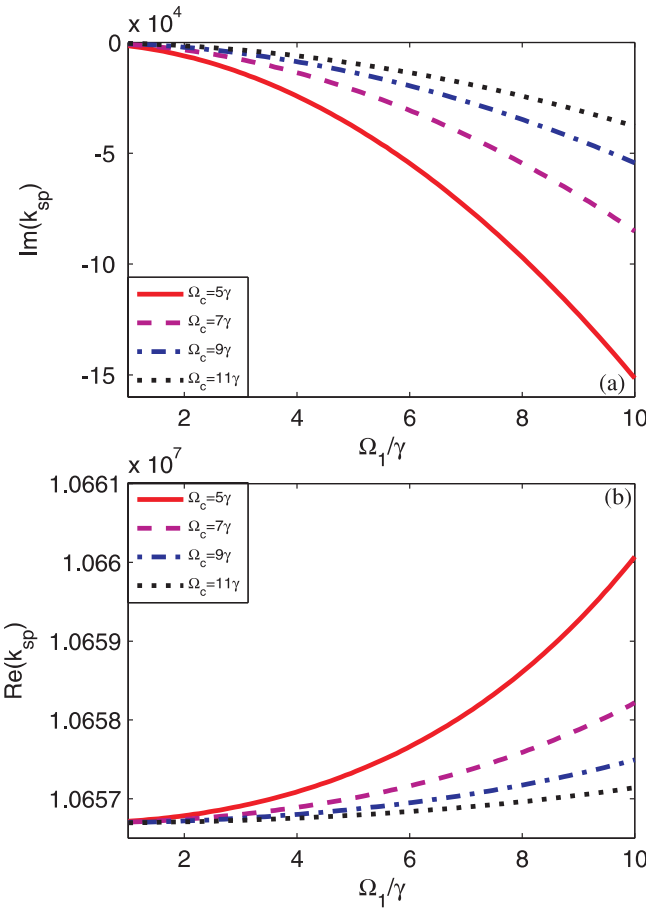


FIG. 4. Variation of the SPP wave vector  $k_{sp}$  (in  $\text{m}^{-1}$ ) with pump field Rabi frequency  $\Omega_1$  for (a) the imaginary part and (b) the real part of  $k_{sp}$ . The spectral parameters in (a) and (b) are  $\gamma_{ac,ad,bd} = 2.5\gamma$ ,  $\gamma_{ab,cd} = 0.5\gamma$ ,  $\Delta_{p,1} = 30\gamma$ ,  $\Omega_c = 5\gamma$  (red solid line),  $\Omega_c = 7\gamma$  (magenta dashed line),  $\Omega_c = 9\gamma$  (blue dash-dotted line),  $\Omega_c = 11\gamma$  (black dotted line),  $\varphi_{1,2,3} = \pi/2$ , and  $|\sigma| = 63 \times 10^6 \text{ S/m}$ .

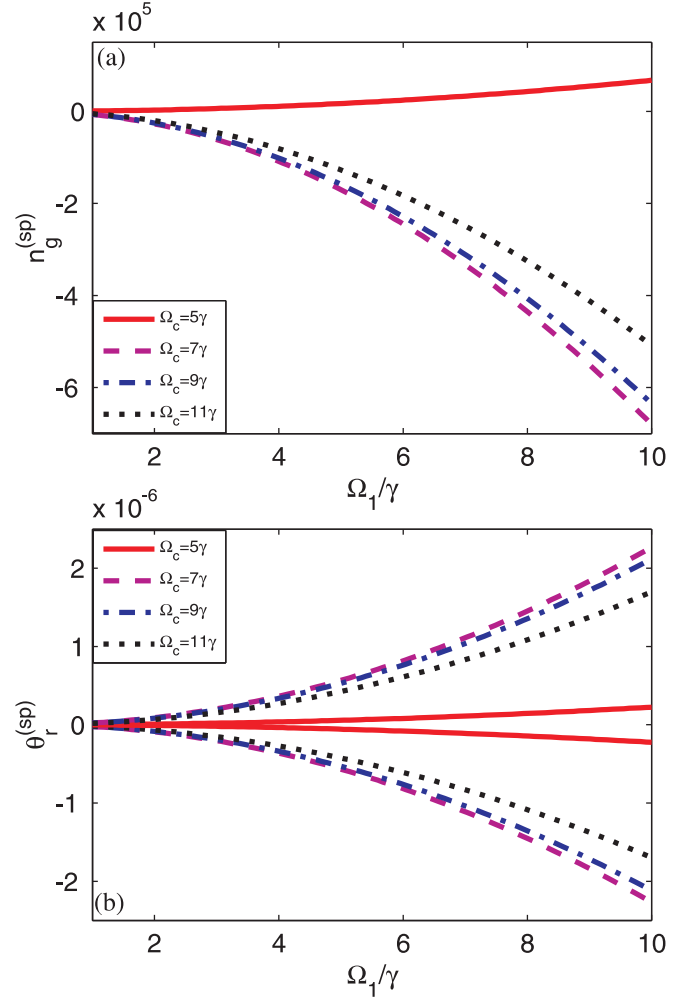


FIG. 5. Variation in (a) the group index and (b) the rotary SPP drag with pump field Rabi frequency  $\Omega_1$ . The parameters are for both (a) and (b)  $\gamma_{ac,ad,bd} = 2.5\gamma$ ,  $\gamma_{ab,cd} = 0.5\gamma$ ,  $\Delta_{1,p} = 30\gamma$ ,  $\varphi_{1,2,3} = \pi/2$ ,  $\Omega_c = 5\gamma$  (red solid line),  $\Omega_c = 7\gamma$  (magenta dashed line),  $\Omega_c = 9\gamma$  (blue dash-dotted line),  $\Omega_c = 11\gamma$  (black dotted line),  $\omega_s = \pm 20 \text{ rps}$ , and  $|\sigma| = 63 \times 10^6 \text{ S/m}$ .

the SPP is  $\pm 2.269 \times 10^{-6}$  rad at  $\Omega_1/\gamma = 10$  and  $\Omega_c = 7\gamma$  (magenta dashed line).

The dependence of the group index of the SPP and its rotary drag on the control field's Rabi frequency is demonstrated in Fig. 6 for various fixed values of probe detuning  $\Delta_p$  at fixed  $\Omega_1 = 2.5\gamma$  while taking the other spectral parameters to be the same as in Fig. 5. The maximum value of the negative group index is  $4.331 \times 10^4$  at  $\Omega_c/\gamma = 7.55$  and  $\Delta_p = 30\gamma$  (red solid line). The corresponding rotary drag of the SPP is  $\pm 1.445 \times 10^{-7}$  rad. Again, the opposite signs of the rotary drag and of the angular speed of the collective medium manifest the superluminal propagation of the SPP.

Analogous to Fig. 3 for the rotary drag of the photon, Fig. 7 demonstrates the rotary drag of the SPP with respect to the rotation speed of the collective structure. Although the trend of the SPP drag is identical to that of the photon drag, the maximum rotary drag of the photon is about  $9.438 \times 10^{-6}$  rad (see Fig. 3) while maximum rotary drag of the SPP is  $\pm 7.508 \times 10^{-7}$  rad at  $\Omega_1 = 8.5\gamma$  and  $\omega_s = \mp 20 \text{ rps}$  (black

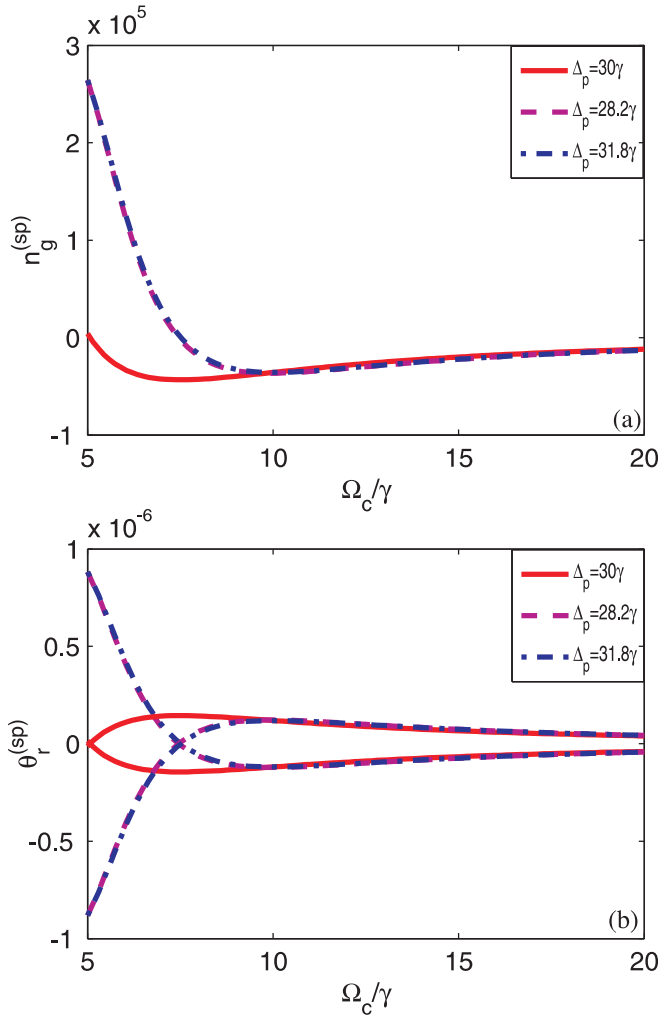


FIG. 6. Variation in the group index and rotary SPP drag with control field Rabi frequency  $\Omega_c$  for (a) the SPP group index and (b) the SPP drag. The other parameters are  $\gamma_{ac,ad,bd} = 2.5\gamma$ ,  $\gamma_{ab,cd} = 0.5\gamma$ ,  $\Delta_1 = 30\gamma$ ,  $\Omega_1 = 2.5\gamma$ ,  $\varphi_{1,2,3} = \pi/2$ , and  $|\sigma| = 63 \times 10^6$  S/m.

dotted line). The difference stems from the corresponding changes in the group index. For fixed spectral parameters, the rotary drag of the SPP  $\theta_r^{SP}$  increases with  $\omega_s$ .

To further elaborate the propagation and rotary drag of the SPP in contrast to that of the photon as in Fig. 2, we include the plot shown in Fig. 8. As one can observe, the two plots reflect an identical trend in the superluminal light propagation both as a photon and as a SPP (e.g., both experience negative group index). However, owing to about 10 times reduction in the value of the group index of the SPP (maximum  $n_g^{SP} = -5.006 \times 10^5$ ) at  $\Omega_c = 7.55\gamma$  and  $\Omega_1 = 8.5\gamma$  (black dotted line), the corresponding rotary drag of the SPP  $\theta_r^{SP}$  is reduced accordingly with a maximum calculated magnitude of  $1.67 \times 10^{-6}$  rad in contrast to that of  $2.099 \times 10^{-5}$  rad for the rotary drag of the photon.

Regarding the physicality of the predicted results, we believe the effects can be tested experimentally as the modified spectral parameters, such as the probe field's wavelength, the medium's length, and the density, correspond to realistic

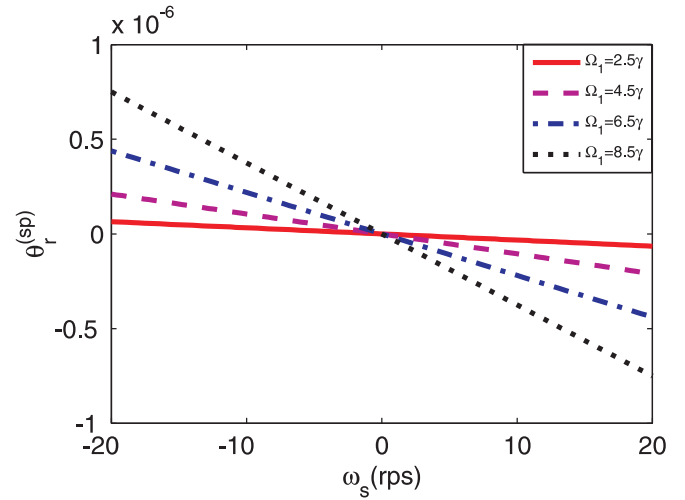


FIG. 7. Dependence of SPP drag on rotation velocity of the atomic-metal interface. The other spectral parameters are  $\gamma_{ac,ad,bd} = 2.5\gamma$ ,  $\gamma_{ab,cd} = 0.5\gamma$ ,  $\Omega_3 = 5.5\gamma$ ,  $\Delta_{p,1} = 30\gamma$ ,  $L = 50 \mu\text{m}$ ,  $\varphi_{1,2,3} = \pi/2$ , and  $|\sigma| = 63 \times 10^6$  S/m.

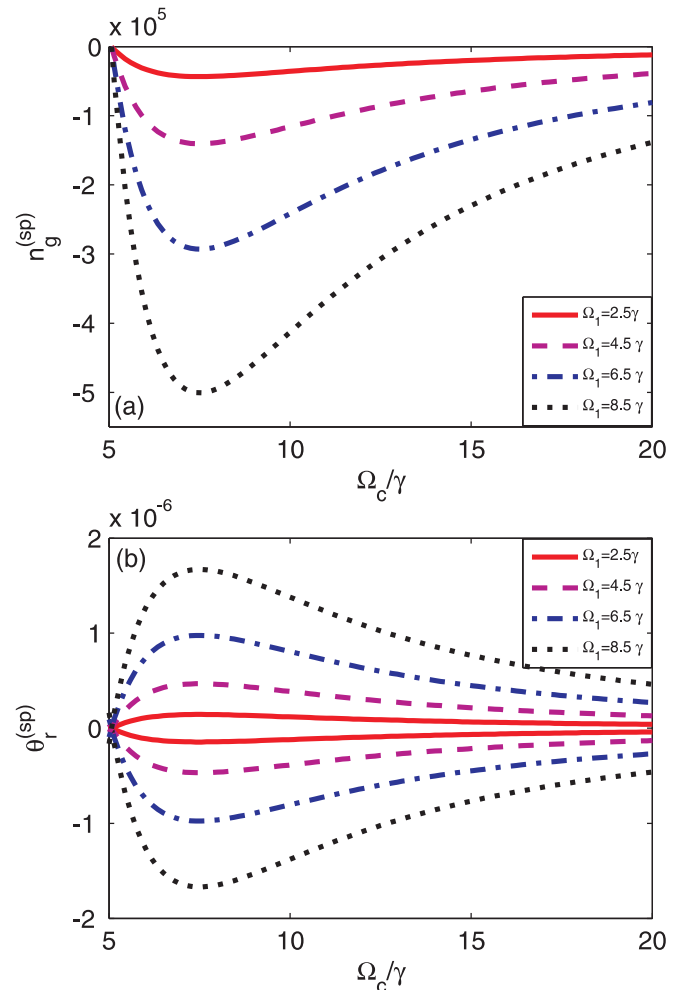


FIG. 8. Impact of control field Rabi frequency  $\Omega_c$  on the group index and the rotary SPP drag for (a) the group index and (b) the SPP drag. The other fixed parameters are  $\gamma_{ac,ad,bd} = 2.5\gamma$ ,  $\gamma_{ab,cd} = 0.5\gamma$ ,  $\Delta_{p,1} = 30\gamma$ ,  $\varphi_{1,2,3} = \pi/2$ ,  $\omega_s = \pm 20$  rps, and  $|\sigma| = 63 \times 10^6$  S/m.

physical systems (e.g.,  $^{23}\text{Na}$  condensate). In particular, the predicted small values of the rotary photon drag of the order of  $10^{-6}$  rad, which stems from the rotation of the polarization state of light in the rotating medium, can be measured by some different experiments such as that devised by Lintz *et al.* [4]. Jones's experiment, with a typical dielectric material, measured the rotation angle on the order of  $5 \times 10^{-6}$  rad [5]. Furthermore, Arnold *et al.* observed an enhancement of the rotary photon drag in a slow-light dielectric medium [6]. The retarding angle of light polarization can also be enhanced considerably by incorporating the anisotropic nature of the rotating optical medium [7]. Regarding the gain coefficient, some researchers have reported measurement of a large gain for various media (see, for example, [8–13]).

### III. CONCLUSION

In this Reply we have corrected several spectral parameters which led to unphysical effects on the gain-assisted superluminal propagation and rotary drag of photons and SPPs [1,2], as pointed out by Macke and Ségard in the preceding

Comment [3]. After incorporating the corrected parameters, the predictions of our theoretical analysis on the gain-assisted superluminal propagation and rotary drag of the photon and that of surface plasmon polaritons have been improved to a good degree of accuracy while keeping the functional form of the interested physical quantities such as the susceptibility, refractive and group indexes, wave vector, and rotary drag of the photon and SPP with respect to the corresponding spectral parameters almost the same as in Refs. [1,2]; so does the main theme or trend of the gain-assisted superluminal propagation and rotary drag of the photon and SPP, however, with predicted effects of an order of magnitude smaller according to the corresponding change in parameters. In addition, the predicted effects are based on the parameters of real physical systems and as such are expected to be tested experimentally.

### ACKNOWLEDGMENT

The authors acknowledge gratefully the useful comments of the referee.

- 
- [1] N. Khan, B. A. Bacha, A. Iqbal, A. Ur Rahman, and A. Afaq, *Phys. Rev. A* **96**, 013848 (2017).
  - [2] N. Khan, B. Amin Bacha, A. Iqbal, A. Ur Rahman, and A. Afaq, *Phys. Rev. A* **96**, 049906 (2017).
  - [3] B. Macke and B. Ségard, preceding Comment, *Phys. Rev. A* **99**, 057801 (2019).
  - [4] M. Lintz, J. Guéna, and M.-A. Bouchiat, *Eur. Phys. J. A* **32**, 525 (2007).
  - [5] R. V. Jones, *Proc. R. Soc. London Ser. A* **349**, 423 (1976).
  - [6] S. Franke-Arnold, G. Gibson, R. W. Boyd, and M. J. Padgett, *Science* **333**, 65 (2011).
  - [7] V. O. Gladyshev, D. I. Portnov, V. L. Kautz, and E. A. Sharandin, *Opt. Spectrosc.* **115**, 349 (2013).
  - [8] D. Wang, C. Liu, C. Xiao, J. Zhang, H. M. M. Alotaibi, B. C. Sanders, L.-G. Wang, and S. Zhu, *Sci. Rep.* **7**, 5796 (2017).
  - [9] G. Vieux *et al.*, *Sci. Rep.* **7**, 2399 (2017).
  - [10] K. Osvay *et al.*, *Appl. Phys. Lett.* **80**, 1704 (2002).
  - [11] D. B. Li and C. Z. Ning, *Phys. Rev. B* **80**, 153304 (2009).
  - [12] Y. Wang, Z. Zhou, J. Yablon, and S. Shahriar, *Opt. Eng.* **54**, 057106 (2015).
  - [13] P. Berini and I. D. Leon, *Nat. Photon.* **6**, 16 (2012).